

2D solar modeling

P. Ventura¹ • V. Penza² •
L. Li, S. Sofia, S. Basu and P. Demarque³

© Springer-Verlag ●●●

Abstract Understanding the reasons of the cyclic variation of the total solar irradiance is one of the most challenging targets of modern astrophysics. These studies prove to be essential also for a more climatologic issue, associated to the global warming. Any attempt to determine the solar components of this phenomenon must include the effects of the magnetic field, whose strength and shape in the solar interior are far from being completely known. Modelling the presence and the effects of a magnetic field requires a 2D approach, since the assumption of radial symmetry is too limiting for this topic. We present the structure of a 2D evolution code that was purposely designed for this scope; rotation, magnetic field and turbulence can be taken into account. Some preliminary results are presented and commented.

Keywords Sun: evolution — Sun: interior

1 Introduction

It is well known that the Total Solar Irradiance (TSI) varies with time, with variations both on a short time scale, of the order of days to months, and on a long time scale, which follows the 11-years solar cycle (Willson & Hudson 1991). While the short-term variations are associated to the solar rotation, as a consequence of surface spots and faculae, which determine

the variation of the energy flux in the Earth's direction, the reasons for the long-term variation are more debated, as confirmed by the extensive literature in that regard, ranging from a more "surface" interpretation (Krivova et al. 2003) to papers stressing the role of a possible variation of the internal structure of the Sun (Li & Sofia 2001).

In this latter case we would expect that at least the whole convective envelope is involved, thus opening the possibility of variability on even longer time scales which could drive long-term variations of the Earth's climate on the Earth. This confirms the importance of understanding the role played by the internal variation of the solar structure.

Among all the possible causes that may potentially alter periodically the solar structure, the magnetic field is generally regarded as the main contributor. Some preliminary investigations, limited to a 1D treatment, and thus limited to purely radial symmetry configurations, showed that the observed variation of the TSI can be reproduced by assuming the presence of a large-scale magnetic field, which varies in phase with the solar cycle (see e.g. Li & Sofia (2001)).

The 1D approach unfortunately proves to be of extremely limited relevance for such an important investigation, because any realistic model of the Sun, accounting for rotation and magnetic field, is expected to develop asymmetries at least of the order of magnitude of the effects that we want to investigate. Also, it is practically impossible to find any morphology of the magnetic field that is radially symmetric, whatever its toroidal or poloidal components are.

These arguments stimulated our group to take a step further, with the extension of the classic YREC code for stellar evolution (Demarque et al. 2008) to a 2D structure, accounting for variations of the main physical and chemical quantities not only with the distance from the center, but also with the latitude. In this

P. Ventura

INAF - Observatory of Rome, Via Frascati 33, 00040 Monte Porzio Catone, Italy

V. Penza

Università di Roma "Tor Vergata", Via della ricerca scientifica 1, 00133 Roma, Italy

L. Li, S. Sofia, S. Basu and P. Demarque

Department of Astronomy, Yale University, P.O. Box 208101, New Haven, CT 06520-8101, USA

paper we describe the theoretical framework that introduces bidimensionality, and that accounts for the effects of magnetic fields, turbulence and rotation; we eventually provide a new set of differential equations that must be solved to determine the solar structure, and the changes expected when the above mentioned phenomena are considered.

The paper is organized as follows: Sections 2 and 3 review the modifications to the standard stellar structure equations needed to involve a magnetic field and turbulence; the structure of the 2D code, with the relevant equations, is presented in Section 4. Some preliminary results are given in Section 5.

2 The inclusion of magnetic field in stellar modeling

The effects due to the presence of an internal magnetic field are modeled following the method described in Lydon & Sofia (1995). The magnetic field is described by means of an energy density $\chi_m = B^2/8\pi\rho$. We list hereafter all the modifications demanded to properly account for the presence of this perturbation.

1. The total pressure is

$$P_T = P_{\text{gas}} + P_{\text{rad}} + \frac{B^2}{8\pi}$$

where the magnetic contribution was added to the standard gas and radiation components.

2. The equation of state (EOS) is consequently changed, as density depends not only on pressure and temperature, but also on the strength of the magnetic field:

$$d \ln \rho = \alpha d \ln P_T - \delta d \ln T - \nu_m d \ln \chi_m$$

where $\alpha = d \ln \rho / d \ln P_T$, $\delta = d \ln \rho / d \ln T$, $\nu_m = d \ln \rho / d \ln \chi_m$

3. The momentum equation must include a magnetic term expressing the Lorentz force, that is

$$\frac{1}{4\pi}(\nabla \times B) \times B = -\nabla \cdot \left(\frac{B^2}{8\pi} \right) + \frac{1}{4\pi}(B \cdot \nabla)B$$

Regarding the anisotropic pressure term $\mathcal{H} = \nabla \cdot (B \cdot B)/(4\pi\rho)$, the latter equation becomes:

$$\frac{1}{4\pi}(\nabla \times B) \times B = -\nabla(P_m) + \rho\mathcal{H}$$

4. The variation of the total entropy S_T , in agreement with the first law of Thermodynamics, must include not only the variation of the internal energy and the

work done by the gas to expand, but also the variation of the magnetic energy density. Expressed differentially, the law giving dS_T becomes

$$TdS_T = dU + PdV + d\chi_m$$

5. The adiabatic gradient ∇_{ad} , defined as the logarithmic derivative of temperature with respect to pressure along a transformation at constant entropy, must change, since the entropy itself contains a new magnetic term. The complete expression is

$$\nabla_{\text{ad}} = \frac{\delta}{\rho c_P} \left(1 - \frac{\nu_m}{\alpha} \nabla_m \right)$$

where $\nabla_m = d \ln \chi_m / d \ln P$.

6. The change in the EOS determines an alteration of the criterion for radiative stability, because the latter is based on the evaluation of buoyancy acting on a convective eddy. The new formulation of the Schwarzschild criterion is

$$\nabla_{\text{rad}} < \nabla_{\text{ad}} \left(1 - \frac{\nu_m}{\alpha} \nabla_m \right)$$

We note that the presence of a magnetic field with a strong gradient in the proximity of the formal border of convection may potentially alter the location of the convection/radiation boundary.

7. The expression for the convective flux is changed in the presence of a magnetic field. Within the context of the Mixing Length Theory (MLT) modelling of convection (Vitense 1953), the convective flux $F_C = \rho v_{\text{conv}} dQ$ is evaluated on the basis of dQ , i.e. the excess heat of the convective eddy with respect to the environment before dissolving: according to expression for the change of the total entropy given in point 4 above, inclusion of possible differences in the magnetic energy density is required. A further modification to the calculation of the convective flux is needed in the evaluation of the convective velocity, made on the basis of the work done by buoyancy: in this case the excess density is not only related to the excess temperature, but also on the different χ_m between the convective element and the environment (see point 2 above).

The above changes were used by Li & Sofia (2001) to perform a qualitative study of the effects of the presence of a large scale magnetic field, allowed to change periodically with the solar cycle, on the global changes of the solar structure. They could reproduce the observed 0.1% variation of the solar luminosity with various magnetic fields, differing in intensity and in the region where they peak. The main results of this first investigation was that deeper magnetic fields required higher intensity, and

were associated to stronger variation of the total radius of the Sun, than shallower ones.

3 The role of turbulence

From the numerical point of view, the inclusion of the effects of turbulence is qualitatively similar to considering the presence of a magnetic field. The key quantities in this context are the turbulent kinetic energy $\chi_t = v^2/2$, and the degree of anisotropy, commonly expressed via the variable $\gamma_t = 1 + 2(v_r/v)^2$. The presence of turbulence also adds a new term to the pressure, i.e. $P_t = \rho(\gamma_t - 1)\chi_t$.

The modifications necessary to include turbulence are the same as those given in the previous section, provided that χ_m and P_m are replaced, respectively, by χ_t and P_t , and that the variation of density in the EOS is expressed in terms of $d\chi_t$ and $d\gamma_t$. The magnetic energy gradient ∇_m is replaced by $\nabla_t = d\ln\chi_t/d\ln P$ in the evaluation of the adiabatic gradient and the super-adiabaticity, and in the Schwarzschild criterion.

The momentum equation is changed accordingly, the two additional terms associated to turbulence being an isotropic pressure component and an anisotropic term, namely

$$-\nabla(P_t) + \rho\mathcal{T}$$

where

$$\mathcal{T} = \nabla \cdot [\rho(v_r v_r - v_\theta v_\theta)e_\theta e_\theta + \rho(v_r v_r - v_\phi v_\phi)e_\phi e_\phi]/\rho$$

In the previous expression we have indicated the three components of the turbulent velocity with v_r , v_θ , and v_ϕ , while $e_\theta e_\theta$ and $e_\phi e_\phi$ are two of the three components of the unit tensor \mathbf{I} .

On the basis of the numerical simulations by Robinson et al. (2001), which give the values of χ_t and γ_t in the superadiabatic layer of the Sun, Li et al. (2002) studied the simultaneous effects of magnetic field and turbulence, and they presented various models that could reproduce the cyclic variation of the solar irradiance, and a nice fit of the observed oscillation frequencies, particularly in the 2000-4000 ν Hz regime (see Fig.12 in Li et al. (2002)).

4 The 2D formulation

A 2D treatment is essential for a reliable and physical investigation of the effects of magnetic fields and turbulence on the solar interior, because the 1D study does not allow for a full exploration of realistic magnetic field configurations, and the 2D effects may be of

the same order of magnitude as the perturbations that we want to investigate. In addition, the satellite PICARD, whose launch is scheduled for the end of 2009, is expected to detect other 2D observational features, which can also be used to discriminate among the various models. These are the reasons behind our choice to develop a full 2D formulation.

Our approach is based on the equipotential surfaces of the gravitational potential, Φ . The mass coordinate is the mass contained within the surfaces $\Phi = const$, which, unlike the 1D case, may not be spherically symmetric. The colatitude θ is the other independent variable. The system is assumed to be azimuthally symmetric. Each equipotential surface is characterized by the expression $r = r(\Phi, \theta)$. The density is generally not constant on the equipotentials; yet, it is possible to introduce an integrated density, defined as

$$\rho_m = \frac{1}{2r^2} \int_0^\pi \rho r^2 \sin\theta d\theta$$

The basic equations used are the canonical relations expressing the equilibrium of the stellar structure, namely the conservation of mass, momentum and energy, and the Poisson equation. Unlike the 1D case, the gradient of the gravitational potential Φ has a transverse component \mathcal{G} , and its radial part deviates by the unknown quantity U from the standard expression, Gm/r^2 :

$$\nabla\Phi = \left(\frac{Gm}{r^2} + U, \mathcal{G} \right)$$

The horizontal component of the energy flux, F_θ , must also be considered, although the luminosity is still related to the radial flux.

In agreement with the discussion of the previous sections, the momentum equation needs modifications with respect to the standard case to account for the presence of magnetic field and turbulence. Rotation generates a centrifugal acceleration that must be included: $\mathcal{R} = \Omega^2 r \sin\theta(\sin\theta, \cos\theta)$

Eventually, these hypotheses lead to a system of 5 differential equations:

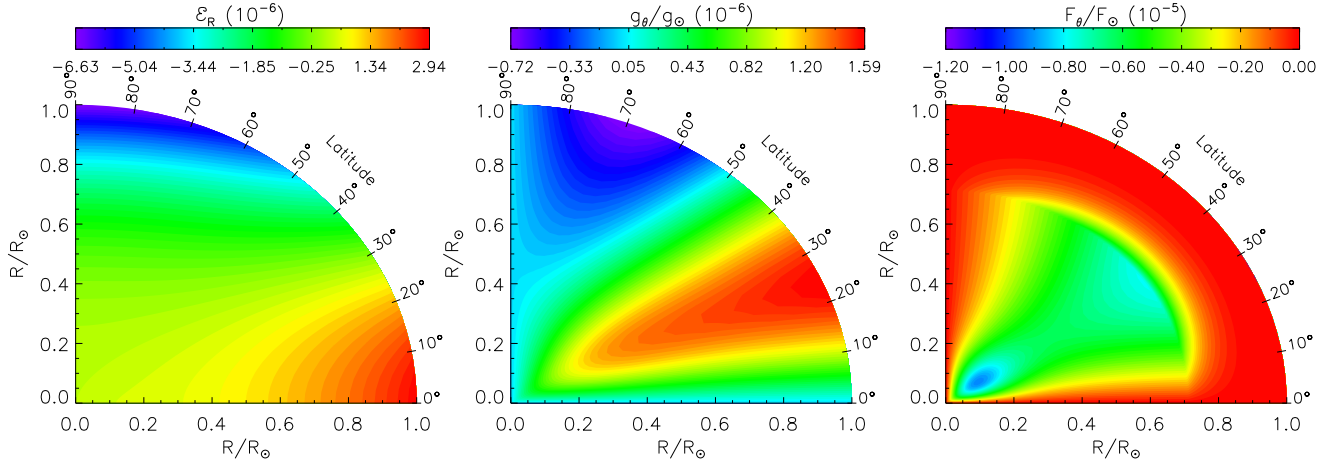


Fig. 1 The structure of a rotating 2D solar model is shown in terms of ϵ_R , i.e. the variation of the radius compared to a non rotating 1D, radially symmetric structure (left), the value of the colatitudinal acceleration g_θ (center), expressed in units of the solar surface gravity g_\odot , and the horizontal flux F_θ (right).

$$\frac{d \ln r}{d \ln m} = \frac{m}{4\pi r^3 \rho_m} \quad (1)$$

$$\frac{d \ln P}{d \ln m} = -\frac{m}{4\pi r^2 P} \frac{\rho}{\rho_m} \left(\frac{gm}{r^2} + U - \mathcal{H}_r - \mathcal{T}_r - \mathcal{R}_r \right) \quad (2)$$

$$\frac{d \ln P}{d \ln m} = \nabla \frac{d \ln T}{d \ln m} \quad (3)$$

$$\frac{dL}{d \ln m} = \frac{m}{L_\odot} \frac{\rho}{\rho_m} \left(\epsilon - T \frac{dS}{dt} \right) - \frac{m F_\theta \cot \theta}{L_\odot r \rho_m} - \frac{m}{L_\odot r \rho_m} \frac{\partial F_\theta}{\partial \theta} \quad (4)$$

$$\frac{dU}{d \ln m} = \frac{Gm}{r^2} \left(\frac{\rho}{\rho_m} - 1 \right) - \frac{m}{4\pi r^3 \rho_m} (2U + \mathcal{G} \tan \theta + \frac{\partial \mathcal{G}}{\partial \theta}) \quad (5)$$

The colatitudinal acceleration, \mathcal{G} , can be found via the horizontal component of the momentum equation and considering the Poisson equation:

$$\mathcal{G} = H_\theta + \mathcal{T}_\theta + \mathcal{R}_\theta - \frac{1}{r} \frac{\partial P}{\partial \theta} \quad (6)$$

The 5 differential equations given above must be integrated from the center to the surface, and from the pole to the equator. Provided that the structure is divided into N mass shell and M angles, the linearization procedure leads to 5(M-1)(N-1) equations for the 5MN unknown, i.e. the values of the 5 variables in the whole star. The system is closed with the following boundary conditions:

- 3(M-1) central conditions, setting $R=L=U=0$ at the centre.

- 2(M-1) boundary conditions at the surface, that express the matching between the integration from the interior and the atmospheric treatment.
- 5N conditions at the pole, i.e. that the 5 variables have null angular gradient at $\theta = 0$.

The need of a high numerical accuracy demands one to find the shape of the equipotential surfaces before the integration of the above systems is performed. This is accomplished by using the condition of hydrostatic equilibrium, based on which we assume that pressure and its derivative with respect to mass are constant along the $\Phi = \text{const}$ surfaces. The interested reader may find in Li et al. (2006) and Li et al. (2009) an accurate description of the numerical structure of the code used, and the techniques adopted to solve the full system of linearized equations.

5 Applications of the 2D scheme

The new formulation for the 2D approach was tested for two simple cases, namely i) a solar model where only the effects of a differential rotation in agreement with the observations of the solar spots is adopted, and ii) a structure where a purely toroidal magnetic field is allowed to vary in phase with the solar cycle. This step, considering the complexity of the numerical treatment requested, is mandatory before more complex magnetic field configurations, in which both the toroidal and the poloidal components are present, are investigated.

5.1 The rotating model

We studied the effects of differential rotation on the solar structure. No turbulence and magnetic field were

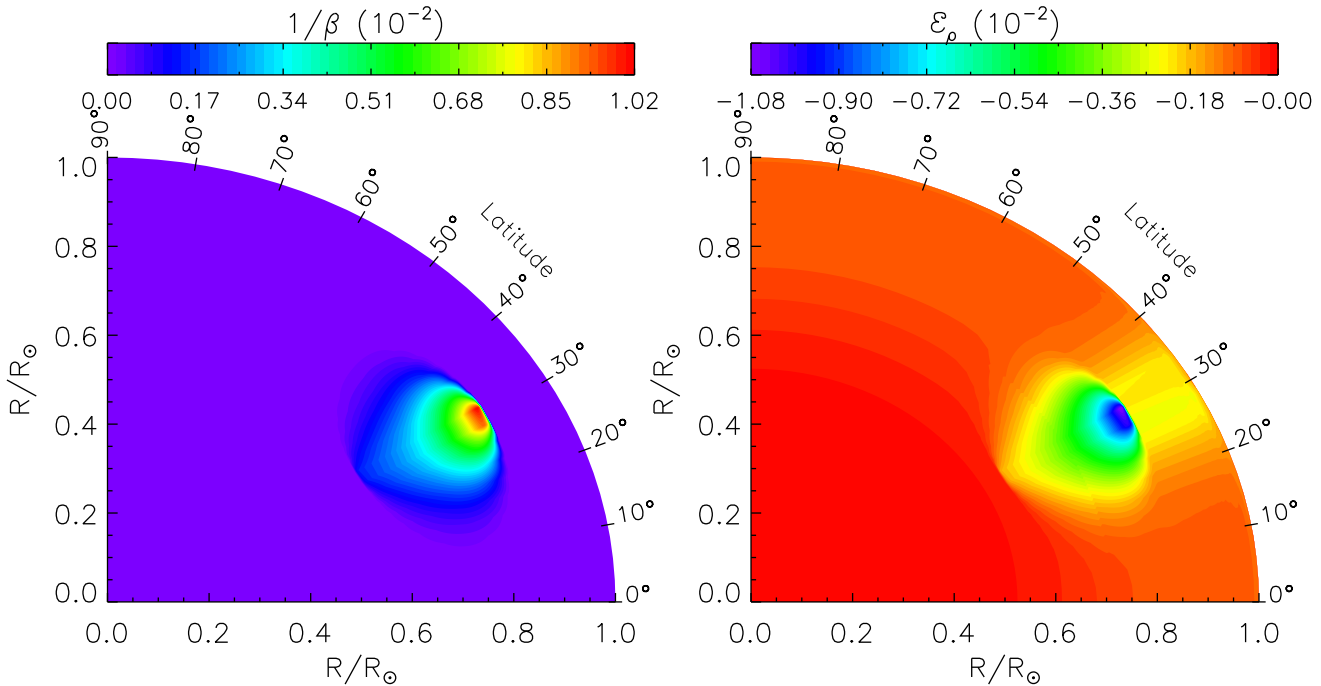


Fig. 2 The structure of a solar model that includes the effects of a toroidal magnetic field. Left: the ratio between the total pressure and the corresponding pressure of a standard 1D model with no magnetic field; right: relative variation of density with respect to the standard model

included. This requires one to neglect the \mathcal{H} and \mathcal{T} terms in eqs.1-5, and to consider only the \mathcal{R} vector, associated with rotation.

The three panels of Fig.1 show the modifications introduced by rotation in comparison with the standard 1D radially symmetric solar model. We focus our attention on those quantities more sensitive to the 2D modeling, i.e. radius (left), colatitudinal acceleration \mathcal{G} (center), and transverse radiative flux, F_θ (right).

The radius variation is easily understood on the basis of the expression for the centrifugal force, which increases from the pole to the equator, thus determining an expansion of the star at high colatitudes, and a contraction at the poles; this is effectively what is observed in the left panel of Fig.1.

The contours for \mathcal{G} , shown in the central panel of Fig.1, can be interpreted on the basis of eq.6 giving the expression for \mathcal{G} . Given the absence of the magnetic and turbulent contributions, the value of \mathcal{G} is given by the balance between the centrifugal horizontal term, $\frac{1}{2}\Omega^2 r \sin 2\theta$, and the derivative of pressure with respect to θ calculated along the constant radius surfaces. This latter quantity is always positive, because the expansion of the structure towards the equator makes the $r = \text{const}$ surfaces correspond to higher Φ surfaces (hence, higher pressure) at higher θ . The two terms are therefore of opposite sign, with the centrifugal term dominating close to the equator, where the centrifugal acceleration is higher. \mathcal{G} is thus expected to be positive

close to the equator. The pressure term is the dominant term close to the pole, where, indeed, we see from the central panel of Fig.1 that \mathcal{G} is negative. Note that \mathcal{G} vanishes as the equator is approached, since we expect purely radial contributions of all quantities there.

The profiles of F_θ are associated with the pressure and temperature profiles along the surface at constant radius. Like the pressure, even the temperature is expected to increase moving at constant radius from the pole to the equator; this determines a flux in the opposite direction, i.e. from high- to low- θ regions, which corresponds to a negative horizontal flux, as confirmed by the right panel of Fig.1. Again, we may comment that the effects tend to vanish at the pole and at the equator and in the convective mantle, which is less sensitive to temperature variation than the radiative interior.

The luminosity (not shown) changes accordingly to what is discussed above. We stress the increase/decrease of the radial flux on the equator/pole, which can be directly associated to the behavior of the radius. The nuclear core, as expected, is almost insensitive to rotation.

5.2 Toroidal field

We started to investigate the effects of a magnetic field with a simple configuration, namely a toroidal field with two torus tubes that are parallel to the equatorial plane.

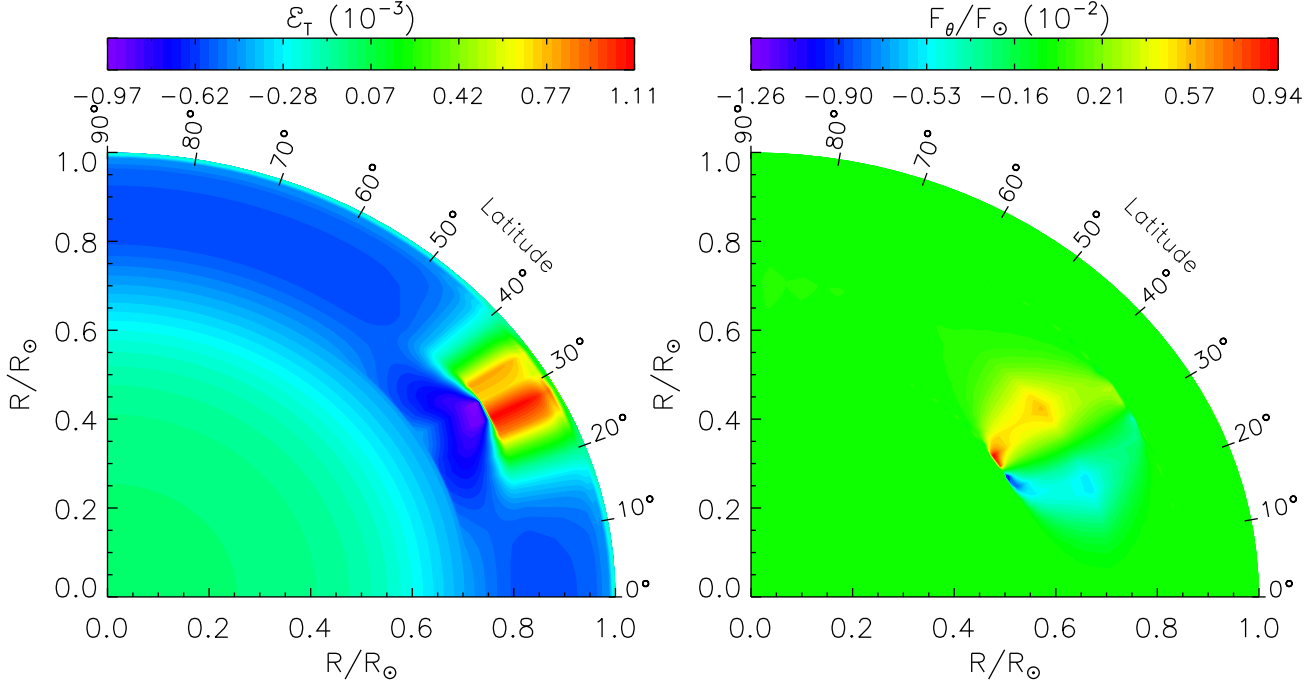


Fig. 3 Left: the same as Fig.2, but indicating the relative variation of temperature; right: the horizontal component of the radiative flux, F_θ .

The field B is assumed to peak in a region close to the bottom of the convective envelope, at a latitude of $\theta = 30^\circ$, and to decay gradually with mass, with a gaussian profile. The region where B is located can be seen in the left panel of Fig.2, showing the ratio between the total pressure (including the magnetic contribution) and the pressure of the standard 1D model, in which rotation, magnetic field and turbulence are neglected.

The right panels of Fig.2 shows the relative variation of density. The density contours confirm that the region where the magnetic perturbation is present expands, due to the hydrostatic equilibrium condition, which demands a drop of the gas pressure. Note that, for continuity reasons, and because of the non-linearity of the stellar structure, wings of these effects reach also zones far away from the perturbation (i.e. the polar regions in the envelope).

The temperature (shown in the left panel of Fig.3), is consequently decreased in the low-density regions, although the surface zone immediately above the perturbation is indeed hotter, as demanded by hydrostatic equilibrium and the drop of density over there. The region where the perturbation is located is thus characterized by a strong horizontal temperature gradient, which is positive (i.e. temperature increases with the colatitude θ) in the higher θ regions, and becomes negative from the peak of the perturbation towards the equator. This consideration allows for a straightforward understanding of the right panel of Fig.3, which

shows a positive transverse flux in the upper part of the region encompassed by the magnetic field, and a negative F_θ at lower latitudes.

6 Conclusions

A full comprehension of the mechanism driving the long-term variation of the total solar irradiance is far from being reached. The debate regarding the possible role played by periodic changes of the internal structure is still open, as confirmed by the many contributions in favor of a completely external solution, and other works stressing the importance to structural changes, most probably associated to a variable large-scale magnetic field.

To understand how the presence of a magnetic perturbation could contribute to the cyclic variation of the TSI, we developed a 2D solar evolution code, the two independent coordinates being the mass enclosed within a given equipotential surface, m , and the colatitude, θ . The full formulation consists in 5 differential equations, to be integrated from the center to the surface, and from the pole to the equator.

We applied this scheme to a test of the effects of a rotating solar model (note that both uniform and differential rotation can be straightforwardly implemented), and to a structure accounting for the presence of a toroidal magnetic field.

More general configurations of the magnetic field will be investigated in future work.

Acknowledgements S.S. acknowledges the support of the G.Unger Vetlesen Foundation, and the Brinson Foundation; L.L.H. acknowledges support by NFS grant ATM-0737770; S.B. by NFS grants ATM-0737770 and ATM-0348837; P.D. by NASA grant NAG5-13299.

References

- Demarque, P., Guenther, D.B., Li, L.H., Mazumdar, A., & Straka, C.W. 2008, *Ap&SS*, 316, 31
- Krivova, N.A., Solanki, S.K., Fligge, M., & Unruh, Y.C. 2003, *A&A*, 399, L1
- Li, L.H., Robinson, F.J., Demarque, P., Sofia, S., & Guenther, D.B. 2002, *Astrophys. J.*, 567, 1192
- Li, L.H., & Sofia, S. 2001, *Astrophys. J.*, 549, 1204
- Li, L.H., Ventura, P., Basu, S., Sofia, S., & Demarque, P. 2006, *Astrophys. J. Suppl. Ser.*, 164, 215
- Li, L.H., Sofia, S., Ventura, P., Penza, V., Bi, S., Basu, S., & Demarque, P. 2009, *Astrophys. J. Suppl. Ser.*, 182, 584
- Lydon, T., & Sofia, S., 1995, *Astrophys. J. Suppl. Ser.*, 101, 357
- Robinson, F.J., Demarque, P., Sofia, S., Chan, K. L., Kim, Y. C., & Guenther, D. B. 2001, *Proc. SOHO 10/GONG 2000 Workshop, Helio- and Astroseismology at the Dawn of the Millenium*, ed. A. Wilson (ESA SP-464; Noordwijk: ESA), 443
- Vitense, E. 1953, *Zs. Ap.*, 32, 135
- Willson, R.C., & Hudson, H.S. 1991, *Nature*, 351, 42